

Molecular Simulation Study of the Effect of Various Additives on Salbutamol Sulfate Crystal Habit

Yin Yani,^{*,†} Pui Shan Chow,[†] and Reginald B. H. Tan^{†,‡}

[†]Institute of Chemical and Engineering Sciences, A*STAR (Agency for Science, Technology and Research), 1 Pesek Road, Jurong Island, Singapore 627833

[‡]Department of Chemical and Biomolecular Engineering, National University of Singapore, 4 Engineering Drive 4, Singapore 117576

ABSTRACT: The effects of polyvinylpyrrolidone (PVP), hydroxypropyl methyl cellulose (HPMC), and lecithin additives on salbutamol sulfate (SS) crystal growth are studied using molecular dynamics (MD) simulation, to provide an insight into the interaction between the additives and SS crystal faces at the atomistic level. The interaction energy between additives and crystal faces is presented. The intermolecular contacts between the additives and the crystal faces are analyzed by calculating the average number of contacts between O atoms of the additives and the H atoms of the first layer of the SS crystal. The mobility of each additive on SS crystal faces is also reported by determining the mean square displacement. Our results suggest that PVP is the most effective among the three additives for the inhibition of SS crystal growth. The methodology used in this study could be a powerful tool for selection of habit-modifying additives in other crystallization systems.

KEYWORDS: molecular dynamics simulations, polymer, additives, crystal habit, salbutamol sulfate, polyvinylpyrrolidone

1. INTRODUCTION

The presence of impurities or additives, even at very small amounts, has long been known to have a major impact on crystallization processes.^{1,2} The impurities and additives can influence the nucleation and growth rates,^{1,3,4} leading to a change in polymorph or crystal habit.^{2,5–8} In industrial crystallization processes, impurities are often present in solutions from upstream processes and are structurally related to the solute molecules.^{2,7} In some cases, additives are intentionally added to exercise some form of control over the crystallization product, e.g. modify the crystal habit^{5,6,9} and to stabilize a metastable polymorph.^{10,11} When the additives are structurally related to the solute molecule, they interact with the crystalline phase stereochemically and are referred to as “tailor-made” additives.⁴ Due to the partial similarity in molecular structures, these additives are able to interact favorably with the host crystal and become incorporated into the crystal lattice. However, the part of the additive molecule that is dissimilar from the solute molecule then protrudes from the crystal surface and provides stereochemical hindrance to the subsequent incorporation of the solute molecules into the crystal, thus hindering the crystal growth process.⁴

Besides small molecular tailor-made additives, polymers and surfactants have also been used to control crystal nucleation and growth¹² and suppress agglomeration.^{13–18} Polyvinylpyrrolidone (PVP) and hydroxypropylmethyl cellulose (HPMC) were found to modify paracetamol crystal habit from polygonal prismatic to rod-shaped, ellipsoidal or spherical crystals depending on the concentration of the additives.¹³ In the crystallization of hydrocortisone acetate, HPMC was found to delay the nucleation

and modify the crystal habit from a well-defined polar prismatic morphology to a wing-shaped morphology.¹⁶ Most recently, Xie et al.¹⁸ attempted to produce micrometer-size salbutamol sulfate (SS) suitable for inhaled drug delivery with the use of polymeric additives and surfactant such as HPMC, PVP K25 and lecithin. Their results showed that PVP K25 was the most effective additive to inhibit the crystal growth and aggregation of SS with the ability of obtaining the target crystal size range of 1–10 μm . These polymeric and surfactant additives, being usually much bigger than and bearing little or no similarity in chemical structure to the solute molecule, are unlikely to be able to incorporate into the crystal lattice in the same way as the tailor-made additives described earlier on. It has been suggested that the modification effect of polymeric additives on crystallization is due to the selective adsorption of the additives at the crystal/solution interface, where the driving force ranges from purely electrostatic to highly specific recognition of crystal phases by the polymer.¹⁷ Tian et al. attributed the modification effect of the polymers tested on the crystallization of nitrofurantoin hydrate to hydrogen-bonding and polymer network properties.¹⁷ Although experimental methods, including HPLC and a variety of solid state spectroscopic techniques, have been employed to unravel the underlying mechanism,^{19–22} capturing the kinetic process that occurs between additive and solute molecule at the atomistic level is still not accessible due partly to the

Received: May 30, 2011

Accepted: August 29, 2011

Revised: August 19, 2011

Published: August 29, 2011

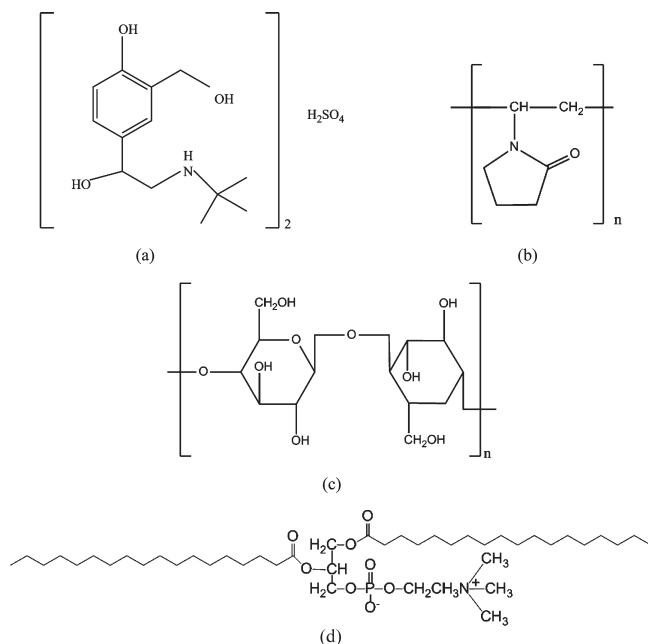


Figure 1. Molecular structure of (a) SS, (b) PVP, (c) HPMC, (d) lecithin.

complexity and the relative weakness of the interactions in aqueous environments, and partly to the limit of detection of the available experimental techniques.

Molecular modeling techniques appear to be a promising way to further our understanding of the interactions between additives and solute molecule.^{4,5,18,23–31} They can be used to probe into details at the atomistic level that may not be accessible by experimental techniques. Among the molecular modeling approaches used, molecular dynamics simulation is able to provide kinetic information of the additive–solute interaction in addition to the static equilibrium configuration and energy calculation.^{24,28,29,32} van Enkevort et al.²⁸ performed Monte Carlo simulations to investigate the impact of tailor-made inhibitors on the growth kinetics of the (001) face of the simple cubic Kossel crystal. Their simulations involved idealized impurity molecules with horizontal and downward bonds similar to those of the growth units in the crystal face and thus may not be applicable to real additives. Hadicke et al.²⁴ studied the effect of polymeric additive on the growth of various calcite crystal faces. The dynamics of the chains of the polymeric additives on the crystal surfaces of calcite were simulated. From the calculated interaction energies between the additives and the calcite substrate and the deformation energies of the additives on the substrate, they concluded that the acrylate-maleate copolymer is a more effective incrustation inhibitor than oligomaleate. Recently, Zhang et al.²⁹ investigated the mechanism by which polymeric additives affect hydroxyapatite crystal growth using a similar molecular dynamics approach. In order to save on computational time and resources, both groups only considered simple model additives consisting of a maximum of 20 monomers rather than a whole polymer chain in their simulations. However, in addition to adsorbing onto the crystal surface and blocking growth site, polymeric additives may form a diffusion barrier at the crystal surface leading to growth inhibition.¹⁶ The longer polymer chains are therefore more efficient in inhibiting crystal growth compared to those with very short chains.²⁴ Simulating the whole polymer chain should provide a more realistic picture to the mode of action of the

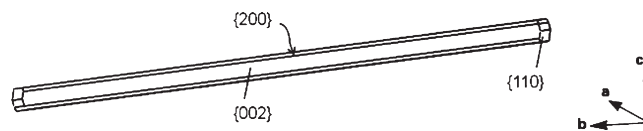


Figure 2. SS crystal morphology predicted with COMPASS force field in Accelrys Materials Studio.⁴⁰

polymeric additive. Therefore, in this work, we performed a detailed molecular dynamics simulation using polymeric additives with chain length matching the real additives used in crystallization.

The model system studied here is salbutamol sulfate, a drug used for the treatment of asthma, chronic pulmonary disease, and other breathing disorders. Xie et al.¹⁸ previously carried out experimental studies to investigate the effect of polymeric additives and surfactants on the crystallization of salbutamol sulfate. They also performed molecular mechanics calculations using a single monomer to represent the polymeric additives. Their experimental data and modeling calculations suggested that PVP adsorbed selectively on the crystal surface via H-bonding formation, thus inhibiting the crystal growth along *b*-axis. It is the aim of this work to further the understanding of the molecular interactions between those additives and the SS crystal faces. By probing into the dynamics of the interaction between the whole polymer chain and the SS crystal faces, we hope to provide direct support to the mechanism proposed by Xie et al.,¹⁸ and provide a general methodology for predicting the inhibitory effects of the additives on SS crystal growth.

2. MOLECULAR MODEL AND METHODOLOGY

The additives considered are PVP K25, HPMC, and lecithin with molecular weight of 25000 g/mol, 10000 g/mol, and 790 g/mol, respectively. The molecular structure of SS and the additives are shown in Figure 1, with $n = 225$ and 62 monomers for PVP and HPMC respectively. The SS crystal structure was obtained from Xie et al.¹⁸ with unit cell dimensions of $a = 27.890$ Å, $b = 6.1857$ Å, $c = 16.760$ Å, $\beta = 98.79^\circ$, and $Z = 4$. The crystal form is monoclinic, and the space group is $C2/c$. As shown in Figure 2, there are three dominant faces of the SS crystal: (200), (110) and (002). As the molecular configurations on (200) and (002) are similar with mainly methyl groups exposed normal to the facet, only (200) and (110) faces are considered in this work. The (200) face was selected and cleaved out of the crystal to a depth of one unit cell, and then the surface was extended to 8×5 unit cells. A 132 Å thick vacuum slab was built above the crystal face. For the (110) crystal face, it was cleaved out to a depth of three unit cells, and the surface was extended to 3×3 unit cells. A 152 Å thick vacuum slab was then built above the crystal face.

Consistent valence force field (CVFF)^{33,34} was used to model the atomic interactions. This force field has been widely used for the molecular simulation study of polymer^{35,36} and other macromolecules.³⁷ In addition, it has been shown that the molecular simulation study using CVFF was able to reproduce the experimental crystal structural parameters of lecithin.^{38,39}

Molecular dynamics (MD) simulations were carried out using the Accelrys Materials Studio (Version 5.0).⁴⁰ During the simulation runs, only the additives were movable, and the crystal surfaces were fixed. The velocity Verlet integrator was used to integrate the equations of motion. The integration time step used was 1 fs. Ewald summation was used to enable the long-range interactions.

Simulation in the NVT (constant number of particle, constant volume, and constant temperature) ensemble was conducted at 600 K for about 6.3 ns to equilibrate and relax a single PVP chain. The same ensemble was also utilized for the simulation of lecithin at 298 K for 1 ns. On the other hand, MD simulation in the NPT (constant number of particle, constant pressure, and constant temperature) ensemble was performed at 1000 K for 2 ns to equilibrate a single HPMC chain. The Nose/Hoover⁴¹ thermostat and barostat were used to control the temperature and pressure, respectively. The relaxed and equilibrated additives were placed randomly on the crystal surfaces. The number of polymer chains or surfactants used was chosen so that the additives can cover the whole surface of the crystal faces studied. Only one polymer chain was employed for PVP and HPMC while twelve molecules were considered for lecithin. MD simulations were then performed for at least 400 ps to ensure that the

structure has equilibrated. Equilibration was determined by observing the change in the thermodynamic properties as a function of time. The equilibrated structures were then minimized with a geometry optimization procedure, and the interaction energies between the additives and the crystal surfaces were obtained by the following expression:

$$E_{\text{interaction}} = E_{\text{total}} - (E_{\text{surface}} + E_{\text{additive}}) \quad (1)$$

in which E_{total} is the total interaction energy of the system (includes all atoms of the first layer of crystal surface and the additive molecule), E_{surface} is the interaction energy of the atoms on the surface, and E_{additive} is the interaction energy of atoms of the additive molecule itself. The possibility of hydrogen bond formation between the crystal surface and the additives was also investigated by calculating the interaction energy between $\text{OH}_{\text{SS_crystal}}$ and the $\text{O}_{\text{additives}}$.

In addition to the interaction energy, the intermolecular contacts of the additives to the crystal faces and the mobility of the additives were also demonstrated at 298 K. The production run for these observations was obtained by carrying out the simulation of the equilibrated systems for another 100 ps at 298 K.

Table 1. The van der Waals Interaction Energy of the Additives on SS Crystal Faces

additive	crystal face	simulations		expts ¹⁸
		van der Waals interactions (kJ/mol)	van der Waals $\text{OH}_{\text{SS_crystal}} \cdots \text{O}_{\text{additives}}$ interactions (kJ/mol)	particle size distribution $d(0.9)$ (μm)
none				80.36 (± 29.78)
PVP K25 (110)		−2158.1	−837.2	6.00 (± 0.02)
HPMC (110)		−595.0	−311.5	30.26 (± 7.39)
lecithin (110)		−2107.9	−394.0	10.68 (± 0.63)
PVP K25 (200)		−1994.9	−674.5	
HPMC (200)		−543.1	−247.2	
lecithin (200)		−1697.0	−391.5	

3. RESULTS AND DISCUSSION

3.1. Intermolecular Interaction Energy between Additives and Crystal Faces. The intermolecular interaction energies between the additives and the SS crystal faces are shown in Table 1. These results give an understanding of the different behavior of additives on the different SS crystal faces. However, due to the absence of solvent molecules in the simulation, the interaction energies calculated only serve as qualitative indicator of the relative inhibitory effects of the additives on crystal growth.

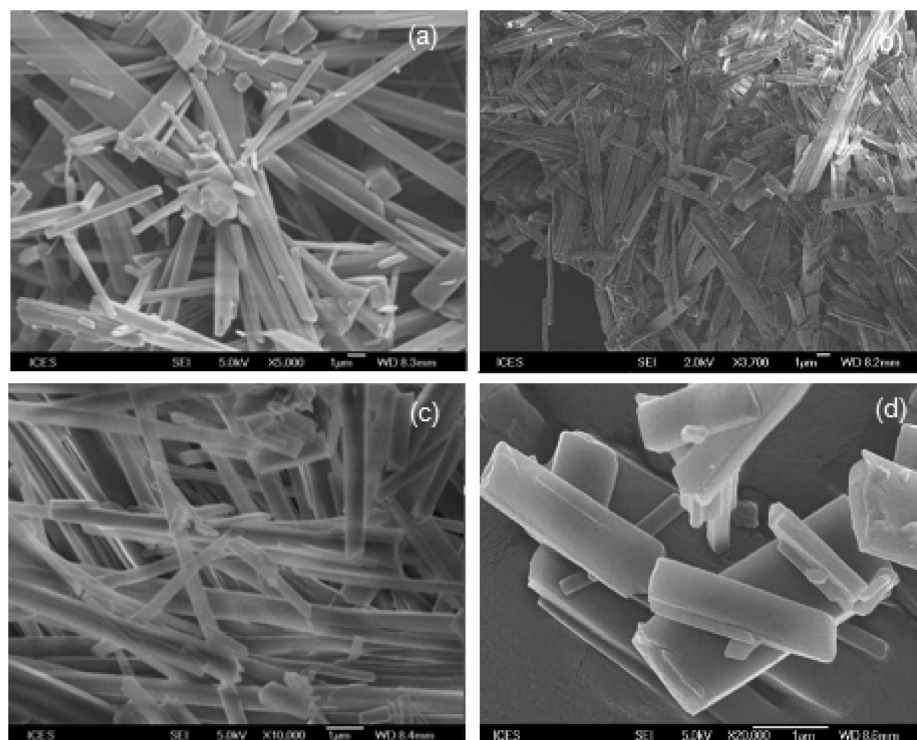


Figure 3. SS crystals obtained at 30 min after nucleation in the presence of (a) no additives, (b) lecithin, (c) HPMC and (d) PVP K25 (adapted from Xie et al.¹⁸).

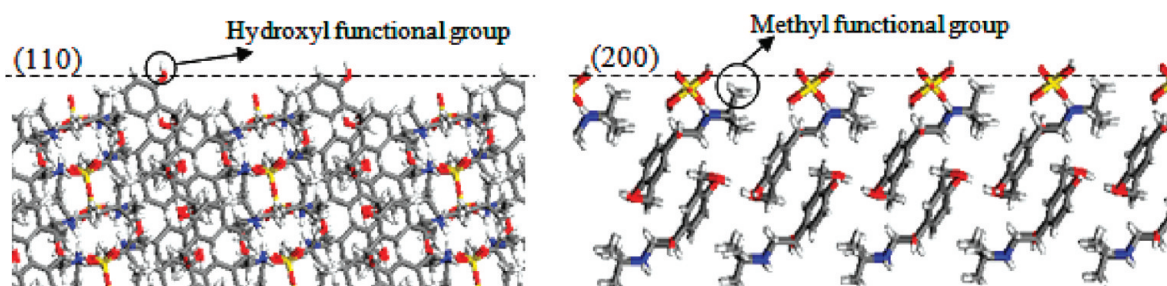


Figure 4. Molecular topology of the $\{110\}$ and $\{200\}$ faces of SS crystals.

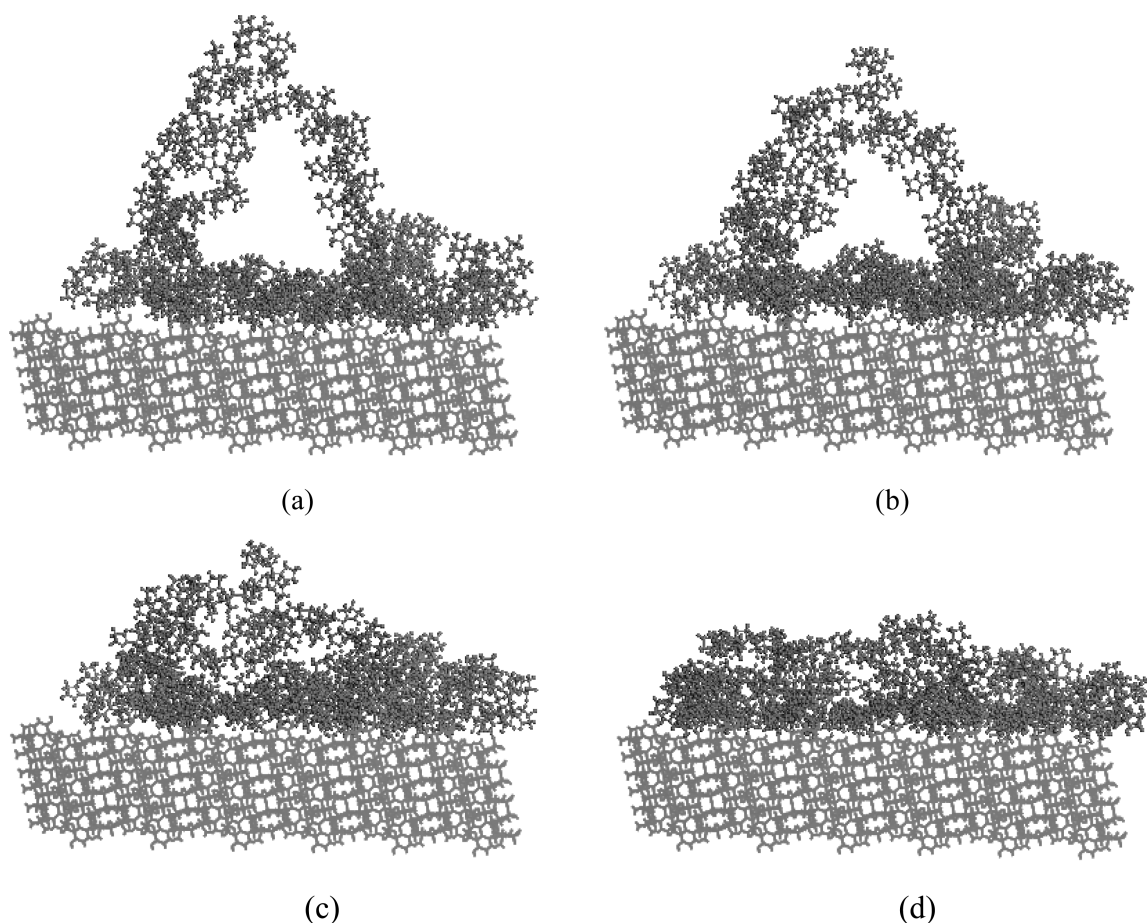


Figure 5. Snapshot of one chain of PVP additive on the (110) SS crystal face at 298 K at (a) 0, (b) 2, (c) 4, and (d) 25 ps.

The main aim in this work was not to calculate accurate quantitative values but to assess and understand the effects of the additives.

In general, PVP has the strongest interaction energy to the SS crystal faces, followed by lecithin and HPMC. This suggests that PVP should be the most effective growth inhibitor. This is indeed in agreement with the experimental results that crystallization in the presence of PVP yielded the shortest $d(0.9)$, followed by lecithin and HPMC (see Table 1). From Table 1, it can also be observed that the intermolecular interaction energy of the additives on the (110) face is generally stronger than the interaction energy on the (200) crystal face. This indicates that the additives have higher tendency to adsorb on (110) than on

(200) thus inhibiting growth along the b direction, and resulting in shorter crystals. This is again in close agreement with the experimental results reproduced in Figure 3.¹⁸ Crystals obtained in the presence of PVP exhibit a much smaller aspect ratio compared to the rest of the additives. Our simulation results have also shown that the interaction energy for HPMC on the (110) face is very similar to that on the (200) face, indicating no significant difference in the direction (a or b) of SS crystal growth retardation by HPMC. This is again evident in the experimental results¹⁸ shown in Figure 3 that crystals in the presence of HPMC maintained the elongated crystal shape, suggesting that the inhibitory effect, if any, is similar in both a and b directions.

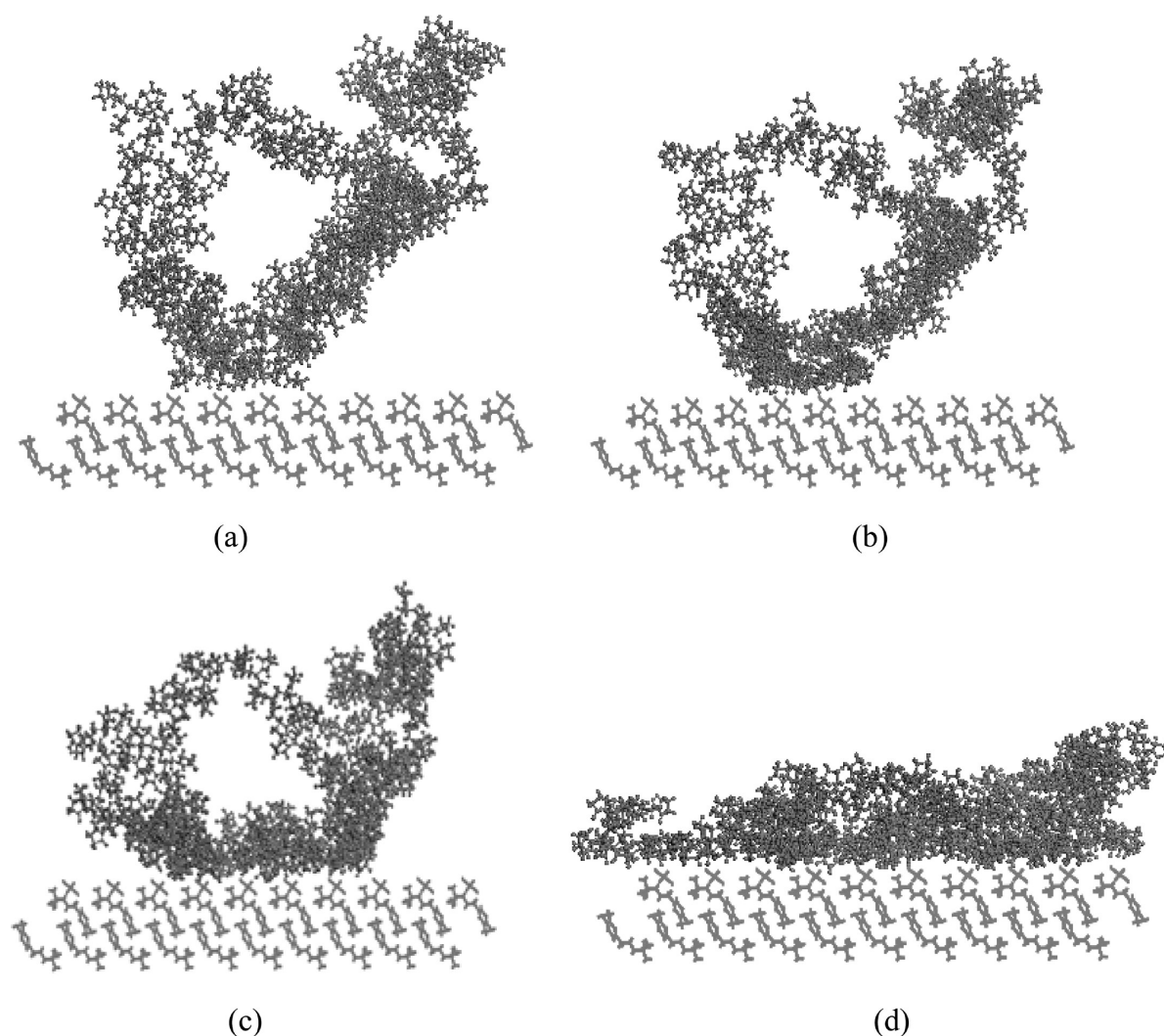


Figure 6. Snapshot of one chain of PVP additive on the (200) SS crystal face at 298 K at (a) 0, (b) 2, (c) 4, and (d) 25 ps.

The tendency of additives to inhibit growth of SS crystal along a certain direction can be explained by the molecular topology on the different faces. Figure 4 shows that on the {200} faces, methyl groups of SS crystal are primarily exposed normal to the facet, resulting in a lack of potential sites to form hydrogen bonds with PVP. However, on the {110} faces, the hydroxyl groups that are bonded to the phenyl ring of the SS molecule are oriented normal to the facet. Therefore, PVP may interact with the SS crystal on this face by forming hydrogen bonds. As shown in Table 1, the van der Waals energy obtained is dominated by hydrogen bond energy which is formed from the intermolecular interaction between oxygen from carbonyl group of PVP and hydrogen of the hydroxyl group of SS on (110) crystal face. Almost 40% of the van der Waals interaction energy for PVP case is contributed by such hydrogen bond energy. Therefore, the interactions due to the $\text{OH}_{\text{SS_crystal}} \cdots \text{O}_{\text{PVP}}$ hydrogen bond play a predominant role in inhibiting crystal growth along the (110) direction, resulting in the change of SS crystal morphology.

3.2. Kinetic Behavior and Conformation of Additives on SS Crystal Faces. Apart from estimating the interaction energy between additives and SS crystal faces, our MD simulations also provide a visualization of the movement of the additive toward the crystal surface as a function of simulation time. Figures 5 and

6 show how the PVP chain approaches and then adsorbs on the (110) and (200) faces, respectively. At 4 ps, almost the whole PVP chain is well distributed on the (110) face. However, at the same time step, it is significantly visible that some fragments of the PVP chain are still quite far away from the (200) crystal face. This indicates that PVP adsorbs faster on the (110) face compared to the (200) face.

In addition, our MD simulation also provides the visualization of how different additives are oriented on the different crystal faces. Figure 7 shows snapshots of the different additives on (110) face at equilibrium at 298 K. Figure 7a demonstrates that O_{PVP} atoms from the carbonyl groups are the majority that bind to the (110) crystal face. This shows that PVP contributes a strong binding affinity due to $\text{OH}_{\text{SS_crystal}} \cdots \text{O}_{\text{PVP}}$ hydrogen bond on the (110) face. This result is in agreement with the energy calculation data in Table 1 that showed hydrogen bond energy being the dominant energy contribution. However, for the HPMC case shown in Figure 7b, the number of O_{HPMC} bounded to the (110) face is far less compared to PVP. The molecular structure of HPMC monomer has hydroxyl and methoxy functional groups which have the ability to form hydrogen bonds with the hydroxyl and amine functional groups of SS. However, due to the steric hindrance of the bulkier methyl

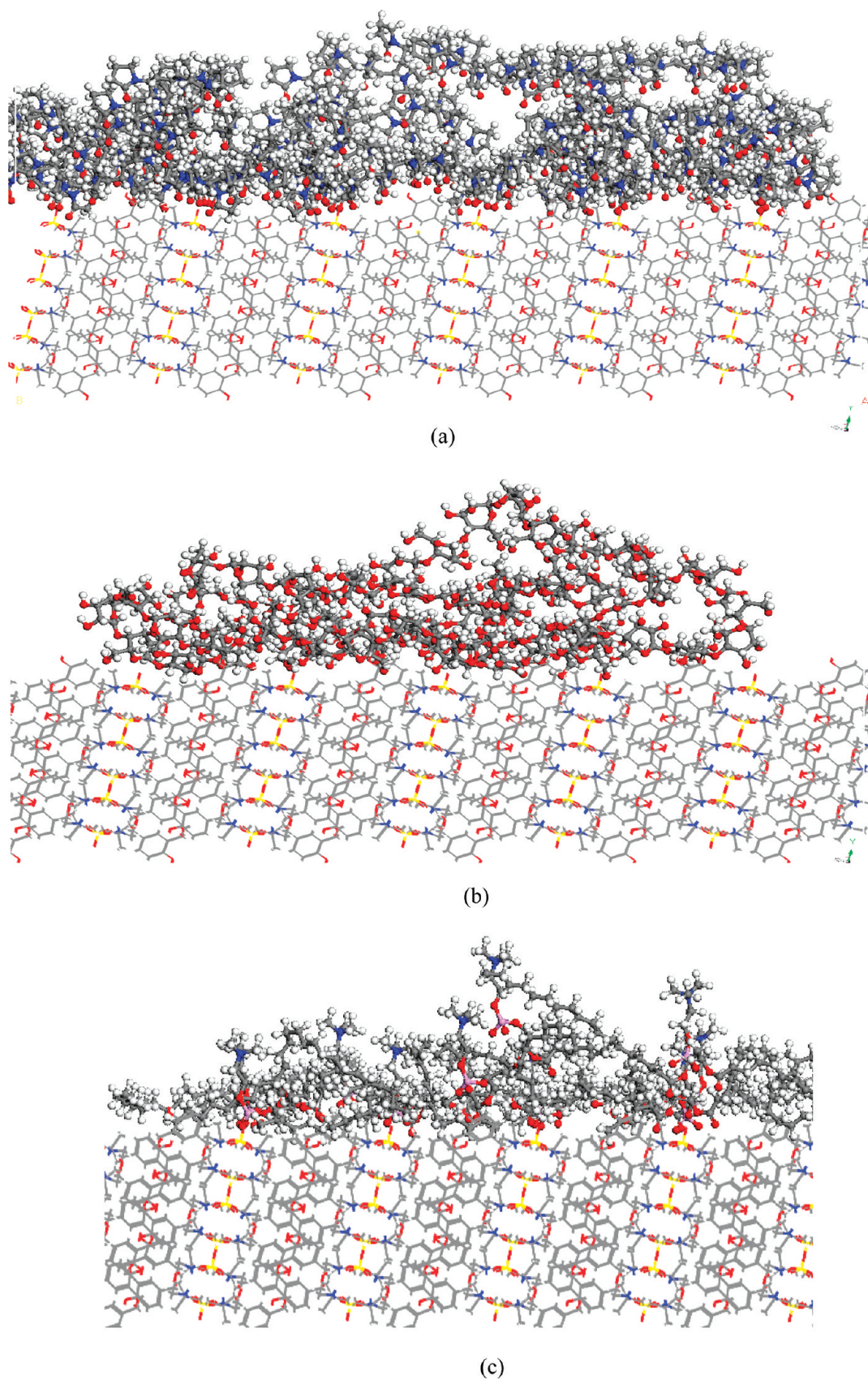


Figure 7. Snapshot of (a) PVP K25, (b) HPMC, and (c) lecithin (red = O, white = H, gray = C, blue = N) on the (110) SS crystal face at equilibrium $T = 298$ K.

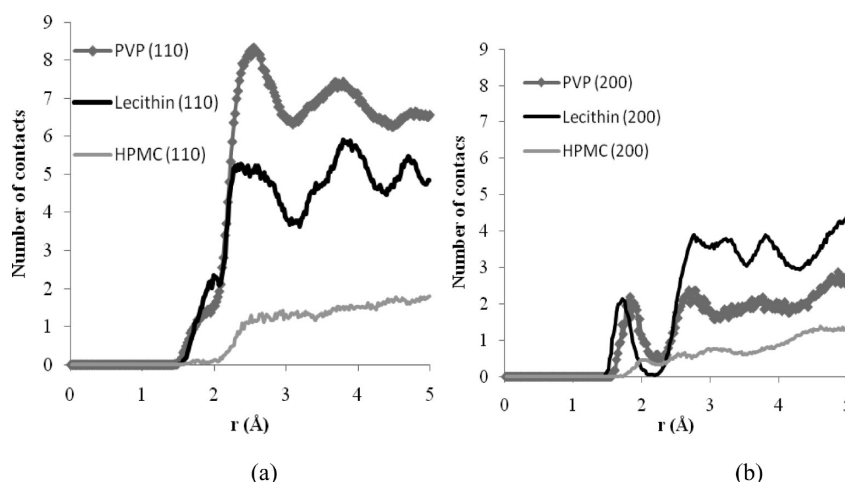


Figure 8. Comparison of the average number of $\text{OH}_{\text{SS_crystal}} \cdots \text{O}_{\text{additives}}$ contacts: (a) (110) face, (b) (200) face.

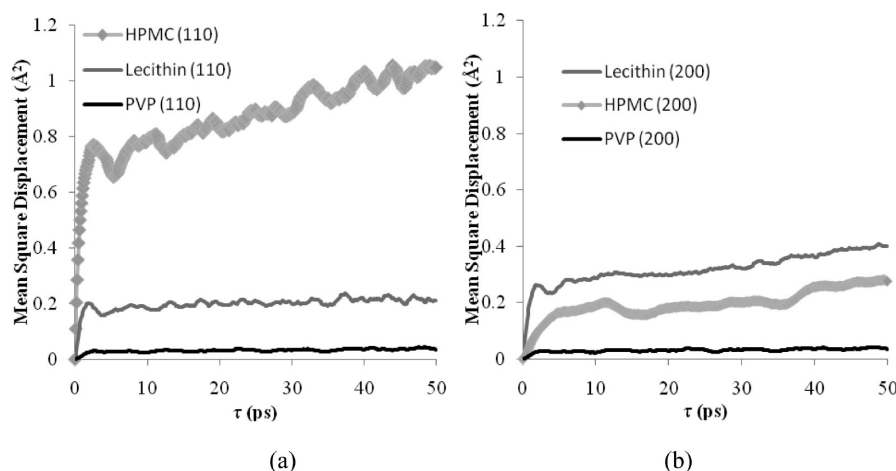


Figure 9. Mean square displacement of additives on the (a) (110) and (b) (200) faces at 298 K.

groups of HPMC, it only has weak interaction with the SS crystal faces and, therefore, does not affect the crystal growth significantly. On the other hand, when lecithin is used as additive (Figure 7c), almost all $\text{O}_{\text{lecithin}}$ atoms from the (PO_3^-) group and from the ($\text{C}=\text{O}$) group bind to the (110) SS crystal face. The close contact of $\text{O}_{\text{lecithin}}$ atoms to the crystal face prevents incorporation of SS molecule onto the crystal face and thus acts as a barrier to the growth of SS crystal at that particular face.

To further analyze the adsorption behavior of the different additives on SS crystal faces, our MD simulations determine the average number of contacts of O atoms of the additives to the H atoms of the first layer of SS crystal in relation to the $\text{OH}_{\text{SS_crystal}} \cdots \text{O}_{\text{additives}}$ distances. Figure 8 shows that the average numbers of $\text{OH}_{\text{SS_crystal}} \cdots \text{O}_{\text{additives}}$ contacts for PVP and lecithin have higher values compared to that for HPMC. This implies that PVP and lecithin have stronger affinity to the SS crystal faces compared to HPMC, and hence may affect the crystal growth more significantly. Balani et al.⁴² recently reported that their infrared spectroscopy (FT-IR) data for the comilled mixtures of amorphous form of SS and PVP showed the formation of strong hydrogen bonds between SS and PVP. This experimental data indicates that PVP has a high propensity to form H-bonds with

SS. Therefore, our results are in good agreement with their experimental observations.

The plot for the PVP case in Figure 8a shows a shoulder at $r \sim 1.8$ Å, followed by a high and distinct peak at $r \sim 2.5$ Å. The shoulder indicates that, within the distances, the number of $\text{OH}_{\text{SS_crystal}} \cdots \text{O}_{\text{PVP}}$ contacts only changes a little. However, the shoulder is not found in Figure 8b; instead, a peak appears. In general, the value of the number of $\text{OH}_{\text{SS_crystal}} \cdots \text{O}_{\text{PVP}}$ contacts for the case of the (110) face is higher compared to that of the (200) face. This indicates that the O_{PVP} has stronger contacts to the (110) face compared to the (200) face, and therefore PVP is more effective in inhibiting the growth of the SS crystal on the (110) face.

The trend of the average number of $\text{OH}_{\text{SS_crystal}} \cdots \text{O}_{\text{lecithin}}$ contacts plot is quite similar to the average number of $\text{OH}_{\text{SS_crystal}} \cdots \text{O}_{\text{PVP}}$ contacts plot. As shown in Figure 8, the values of the number of contacts for lecithin are slightly higher at almost all distances for the case of the (110) face compared to the (200) face. This observation agrees with the interaction energy results that show a small difference between the value of van der Waals $\text{OH}_{\text{SS_crystal}} \cdots \text{O}_{\text{lecithin}}$ interactions energy for the (110) and (200) faces. The flexibility of lecithin may have caused the molecules to move quite easily and, therefore, result in more contacts to both crystal faces.

In addition to the analysis discussed above, our MD simulations also provide the observation of the mobility of additives on SS crystal faces. The analysis was done by determining mean square displacements (MSD) of the additives, expressed in eq 2. The MSDs are calculated based on the center of mass of the additives.

$$\text{MSD} = \langle |r_i(t) - r_i(0)|^2 \rangle \quad (2)$$

where $\langle \dots \rangle$ denotes averaging the number of chains or surfactants used, $r_i(0)$ is the position of the center of mass of the additive at the time origins, and $r_i(t)$ is the position of the center of mass of the additive at time t .

Figure 9 shows that the MSD plot for PVP additive on the (110) crystal face is quite similar to that on the (200) crystal face, indicating a similar degree of PVP mobility on both faces. The MSD values for PVP are much smaller than those for lecithin and HPMC, which means that PVP has the lowest mobility compared to HPMC and lecithin. This analysis supports the results for the interaction energy and the adsorption behavior discussed above. The strong binding affinity of $\text{OH}_{\text{SS_crystal}} \cdots \text{O}_{\text{PVP}}$ reduces the movement of PVP chain on the SS crystal surfaces.

For lecithin, the MSD values for the case of the (110) crystal face are slightly higher than that of the (200) crystal face. This observation again supports the van der Waals $\text{OH}_{\text{SS_crystal}} \cdots \text{O}_{\text{lecithin}}$ interaction energy data that showed only a small difference of the energy value for the case of the (110) and (200) faces.

4. CONCLUSIONS

In this work, we describe the molecular interactions between PVP, HPMC, and lecithin additives and SS crystal faces in atomic scale. Our calculated interaction energy shows that PVP has the strongest interaction energy to SS crystal faces. The average numbers of $\text{OH}_{\text{SS_crystal}} \cdots \text{O}_{\text{additives}}$ contacts have shown higher values for PVP and lecithin compared to that for HPMC. Mean square displacement analysis suggests that the strong binding affinity of $\text{OH}_{\text{SS_crystal}} \cdots \text{O}_{\text{PVP}}$ reduces the movement of PVP chain on the SS crystal surfaces. From the observations, our simulations suggest that PVP is the most effective additive for the inhibition of SS crystal growth, followed by lecithin and HPMC. Our simulations also show that PVP interacted strongly with the (110) faces of SS crystals and therefore predict the growth retardation along the b direction, resulting in shorter crystals. The simulations were able to show that the interactions due to the $\text{OH}_{\text{SS_crystal}} \cdots \text{O}_{\text{PVP}}$ hydrogen bond play a predominant role in inhibiting SS crystal growth. These findings have given a clearer picture to support the mechanism proposed by Xie et al.¹⁸ The methodology used in our study could be a powerful tool for selection of habit-modifying additives in other crystallization systems.

AUTHOR INFORMATION

Corresponding Author

*Institute of Chemical and Engineering Sciences, Crystallisation and Particle Science, 1 Pesek Road, Jurong Island, Singapore 627833. Tel: (65) 6796 3852. Fax: (65) 6316 6183. E-mail: yin_yani@ices.a-star.edu.sg.

REFERENCES

(1) Black, S. N.; Davey, R. J.; Halcrow, M. The kinetics of crystal growth in the presence of tailor-made additives. *J. Cryst. Growth* **1986**, *79* (1–3), 765–774.

(2) Wood, W. M. L. A bad (crystal) habit—and how it was overcome. *Powder Technol.* **2001**, *121* (1), 53–59.

(3) Kubota, N.; Yokota, M.; Mullin, J. W. Supersaturation dependence of crystal growth in solutions in the presence of impurity. *J. Cryst. Growth* **1997**, *182* (1–2), 86–94.

(4) Weissbuch, I.; Lahav, M.; Leiserowitz, L. Toward stereochemical control, monitoring, and understanding of crystal nucleation. *Cryst. Growth Des.* **2003**, *3* (2), 125–150.

(5) Berkovitch-Yellin, Z.; Vanmil, J.; Addadi, L.; Idelson, M.; Lahav, M.; Leiserowitz, L. Crystal morphology engineering by tailor-made inhibitors - a new probe to fine intermolecular interactions. *J. Am. Chem. Soc.* **1985**, *107* (11), 3111–3122.

(6) Poornachary, S. K.; Chow, P. S.; Tan, R. B. H.; Davey, R. J. Molecular speciation controlling stereoselectivity of additives: Impact on the habit modification in alpha-glycine crystals. *Cryst. Growth Des.* **2007**, *7* (2), 254–261.

(7) Poornachary, S. K.; Lau, G.; Chow, P. S.; Tan, R. B. H.; George, N. The effect and counter-effect of impurities on crystallization of an agrochemical active ingredient: Stereochemical rationalization and nano-scale crystal growth visualization. *Cryst. Growth Des.* **2011**, *11* (2), 492–500.

(8) Weissbuch, I.; Zbaida, D.; Addadi, L.; Leiserowitz, L.; Lahav, M. Design of polymeric inhibitors for the control of crystal polymorphism - induced enantiomeric resolution of racemic histidine by crystallization at 25-degrees-C. *J. Am. Chem. Soc.* **1987**, *109* (6), 1869–1871.

(9) Hammond, R. B.; Orley, M. J.; Roberts, K. J.; Jackson, R. A.; Quayle, M. J. An Examination of the Influence of Divalent Cationic Dopants on the Bulk and Surface Properties of $\text{Ba}(\text{NO}_3)_2$ Associated with Crystallization. *Cryst. Growth Des.* **2009**, *9* (6), 2588–2594.

(10) Davey, R. J.; Blagden, N.; Potts, G. D.; Docherty, R. Polymorphism in molecular crystals: stabilization of a metastable form by conformational mimicry. *J. Am. Chem. Soc.* **1997**, *119* (7), 1769–1772.

(11) Stabb, E.; Addadi, L.; Leiserowitz, L.; Lahav, M. Control of polymorphism by 'tailor-made' polymeric crystallization auxiliaries. Preferential precipitation of a metastable polar form for second harmonic generation. *Adv. Mater.* **1990**, *2* (1), 40–43.

(12) Van Eerdenbrugh, B.; Taylor, L. S. Small Scale Screening To Determine the Ability of Different Polymers To Inhibit Drug Crystallization upon Rapid Solvent Evaporation. *Mol. Pharmaceutics* **2010**, *7* (4), 1328–1337.

(13) Femi-Oyewo, M. N.; Spring, M. S. Studies on paracetamol crystals produced by growth in aqueous solutions. *Int. J. Pharm.* **1994**, *112* (1), 17–28.

(14) Murnane, D.; Marriott, C.; Martin, G. P. In situ and Ex situ analysis of salmeterol xinafoate microcrystal formation from poly(ethylene glycol) 400 - Water cosolvent mixtures. *Cryst. Growth Des.* **2008**, *8* (6), 1855–1862.

(15) Paulaine, A. M.; Seyssiecq, L.; Veessler, S. The influence of organic additives on the crystallization and agglomeration of gibbsite. *Powder Technology* **2003**, *130* (1–3), 345–351.

(16) Raghavan, S. L.; Trividic, A.; Davis, A. F.; Hadgraft, J. Crystallization of hydrocortisone acetate: influence of polymers. *Int. J. Pharm.* **2001**, *212* (2), 213–221.

(17) Tian, F.; Baldursdottir, S.; Rantanen, J. Effects of polymer additives on the crystallization of hydrates: a molecular-level modulation. *Mol. Pharmaceutics* **2009**, *6* (1), 202–210.

(18) Xie, S. Y.; Poornachary, S. K.; Chow, P. S.; Tan, R. B. H. Direct precipitation of micron-size salbutamol sulphate - new insight into the action of surfactants and polymeric additives. *Cryst. Growth Des.* **2010**, *10* (8), 3363–3371.

(19) Otsuka, M.; Ishii, M.; Matsuda, Y. Effect of surface-modification on hydration kinetics of nitrofurantoin anhydrate. *Colloids Surf., B* **2002**, *23* (1), 73–82.

(20) Otsuka, M.; Ohfusa, T.; Matsuda, Y. Effect of binders on polymorphic transformation kinetics of carbamazepine in aqueous solution. *Colloids Surf., B* **2000**, *17* (3), 145–152.

(21) Taylor, L. S.; Zografi, G. Spectroscopic characterization of interactions between PVP and indomethacin in amorphous molecular dispersion. *Pharm. Res.* **1997**, *14* (12), 1691–1698.

- (22) Zimmermann, A.; Elema, M. R.; Hansen, T.; Mullertz, A.; Hovgaard, L. Determination of surface-adsorbed excipients of various types on drug particles prepared by antisolvent precipitation using HPLC with evaporative light scattering detection. *J. Pharm. Biomed. Anal.* **2007**, *44* (4), 874–880.
- (23) Clydesdale, G.; Thomson, G. B.; Walker, E. M.; Roberts, K. J.; Meenan, P.; Docherty, R. A molecular modeling study of the crystal morphology of adipic acid and its habit modification by homologous impurities. *Cryst. Growth Des.* **2005**, *5* (6), 2154–2163.
- (24) Hadicke, E.; Rieger, J.; Rau, I. U.; Boeckh, D. Molecular dynamics simulations of the incrustation inhibition by polymeric additives. *Phys. Chem. Chem. Phys.* **1999**, *1* (17), 3891–3898.
- (25) Li, T. L.; Park, K.; Morris, K. R. Understanding the formation of etching patterns using a refined Monte Carlo simulation model. *Cryst. Growth Des.* **2002**, *2* (3), 177–184.
- (26) Mukuta, T.; Lee, A. Y.; Kawakami, T.; Myerson, A. S. Influence of impurities on the solution mediated phase transformation of an active pharmaceutical ingredient. *Cryst. Growth Des.* **2005**, *5* (4), 1429–1436.
- (27) Poornachary, S. K.; Chow, P. S.; Tan, R. B. H. Impurity effects on the growth of molecular crystals: experiments and modeling. *Adv. Powder Technol.* **2008**, *19* (5), 459–473.
- (28) van Enkevort, W. J. P.; Los, J. H. "Tailor-Made" inhibitors in crystal growth: a Monte Carlo simulation study. *J. Phys. Chem. C* **2008**, *112* (16), 6380–6389.
- (29) Zhang, S.-G.; Wang, F.-Y.; Tan, X.-Y. Molecular dynamics simulation on the hydroapatite scale inhibition mechanism of water-soluble polymers. *J. Theor. Chem.* **2010**, *9* (5), 889–902.
- (30) Gupta, P.; Thilagavathi, R.; Chakraborti, A. K.; Bansal, A. K. Role of Molecular Interaction in Stability of Celecoxib–PVP Amorphous Systems. *Mol. Pharmaceutics* **2005**, *2* (5), 384–391.
- (31) Fratev, F.; Jónsdóttir, S. Ó.; Mihaylova, E.; Pajeva, I. Molecular Basis of Inactive B-RAF^{WT} and B-RAF^{V600E} Ligand Inhibition, Selectivity and Conformational Stability: An in Silico Study. *Mol. Pharmaceutics* **2009**, *6* (1), 144–157.
- (32) Liu, H.; Yao, X.; Wang, C.; Han, J., In Silico Identification of the Potential Drug Resistance Sites over 2009 Influenza A (H1N1) Virus Neuraminidase. *Mol. Pharmaceutics* **7** (3), 894–904.
- (33) Dauber-Osguthorpe, P.; Roberts, V. A.; Osguthorpe, D. J.; Wolff, J.; Genest, M.; Hagler, A. T. Structure and energetics of ligand-binding to proteins - escherichia-coli dihydrofolate reductase trimethoprim, a drug-receptor system. *Proteins: Struct., Funct., Genet.* **1988**, *4* (1), 31–47.
- (34) Gaedt, K.; Holtje, H. D. Consistent valence force-field parameterization of bond lengths and angles with quantum chemical ab initio methods applied to some heterocyclic dopamine D-3-receptor agonists. *J. Comput. Chem.* **1998**, *19* (8), 935–946.
- (35) Bhowmik, R.; Katti, K. S.; Katti, D. Molecular dynamics simulation of hydroxyapatite-polyacrylic acid interfaces. *Polymer* **2007**, *48* (2), 664–674.
- (36) Stoliarov, S. I.; Westmoreland, P. R.; Nyden, M. R.; Forney, G. P. A reactive molecular dynamics model of thermal decomposition in polymers: 1. Poly(methyl methacrylate). *Polymer* **2003**, *44* (3), 883–894.
- (37) Mackerell, A. D. Empirical force fields for biological macromolecules: Overview and issues. *J. Comput. Chem.* **2004**, *25* (13), 1584–1604.
- (38) Stouch, T. R.; Ward, K. B.; Altieri, A.; Hagler, A. T. Simulations of lipid crystals - characterization of potential-energy functions and parameters for lecithin molecules. *J. Comput. Chem.* **1991**, *12* (8), 1033–1046.
- (39) Williams, D. E.; Stouch, T. R. Characterization of force-fields for lipid molecules - applications to crystal-structures. *J. Comput. Chem.* **1993**, *14* (9), 1066–1076.
- (40) *Materials Studio Modeling*, 5.02; Accelrys Software Inc.: San Diego, CA.
- (41) Frenkel, D.; Smit, B., *Understanding Molecular Simulation*, 2nd ed.; Academic Press: San Deigo, CA, 2002.
- (42) Balani, P. N.; Wong, S. Y.; Ng, W. K.; Widjaja, E.; Tan, R. B. H.; Chan, S. Y. Influence of polymer content on stabilizing milled amorphous salbutamol sulphate. *Int. J. Pharm.* **2010**, *391* (1–2), 125–136.